*Materials Transactions*, Vol. 52, No. 7 (2011) pp. 1349 to 1355


# Structural Analysis of Pd-Cu-Si Metallic Glassy Alloy Thin Films with Varying Glass Transition Temperature

Susumu Kajita[1], Shinji Kohara[2], Yohei Onodera[3], Toshiharu Fukunaga[3] and Eiichiro Matsubara[4]

[1]*Advanced Materials Development Department, Panasonic Electric Works Co., Ltd., Kadoma 571-8686, Japan*
[2]*Research and Utilization Division, Japan Synchrotron Radiation Research Institute, Kouto, Sayo-cho, Hyogo 679-5198, Japan*
[3]*Research Reactor Institute, Kyoto University, Kumatori-cho, Sennan-gun, Osaka 590-0494, Japan*
[4]*Department of Materials Science and Engineering, Kyoto University, Kyoto 606-8501, Japan*

Thin films of Pd-Cu-Si metallic glassy alloys were fabricated by sputtering method, and the effect of the composition on glass transition temperature ($T_g$) was examined. In order to determine the mechanism of the observed effect, the structural parameters of the thin films based on the short-range order (SRO) were measured, and the correlations between the parameters and the composition were examined. The glass transition temperature ($T_g$) increased with increasing Si and Cu content. The atomic distances (Pd-Si and Pd-Pd) and the coordination number of Si atoms around a Pd atom ($N_{PdSi}$) increased with increasing Si content. The Pd-Pd atomic distance increased with increasing Cu content. These results suggest that Si content and Cu content have positive effect on the formation of a trigonal prism that is reported as a structural unit of Pd-based amorphous alloys. From these observed correlations, it can be concluded that $T_g$ increases with an increase in the formation of a trigonal prism. Therefore, an increase in $T_g$ with increasing Si and Cu content is supposed to be caused by the composition-dependent formation of trigonal prisms. [doi:10.2320/matertrans.M2011023]

(Received January 14, 2011; Accepted April 22, 2011; Published June 15, 2011)

***Keywords:*** *palladium-copper-silicon alloy, metallic glassy alloy, sputtering, thin film, X-ray diffraction, structural analysis*

## 1. Introduction

In recent years, research and development relating to hydrogen energy and fuel cells have been conducted all over the world to solve the environmental problems such as drying up of the fossil fuel and global warming caused by excess amount of $CO_2$ emission. Above all, development of fuel cell vehicles is now in the limelight, and a new type of hydrogen sensor is required for the fuel cell vehicles.[1)]

In order to develop the hydrogen sensor, we adopted a Pd-Cu-Si metallic glassy alloy[2)] for the sensor material, and have reported its excellent hydrogen sensing ability.[3,4)] A metallic glassy alloy is a kind of amorphous alloys, and has glass transition temperature ($T_g$) and wide composition range for forming amorphous phase. It has not grain-boundaries and crystalline defects, resulting in good corrosion resistance and excellent mechanical properties.[5)] In contrast, it will crystallize gradually by receiving heat due to its amorphous structure. If amorphous phase is transformed into crystalline one, its electric resistivity also changes causing inaccuracy for the hydrogen sensor. Therefore, higher $T_g$ is required to prevent the crystallization of a Pd-Cu-Si metallic glassy alloy, because the hydrogen sensor will be used at the temperature of around 373 K. And also, the effect of the composition on $T_g$ should be made clear to determine the optimal composition for the hydrogen sensor material.

For clarifying the effect of the composition on $T_g$ and determining the mechanism, the examination of the correlation between them and the structural analysis are necessary. Several studies on structural analysis of Pd-based amorphous alloys including metallic glassy alloys have been reported previously. Fukunaga *et al.*[6)] have studied the structure of three kinds of amorphous alloys ($Pd_{85}Si_{15}$, $Pd_{80}Si_{20}$ and $Pd_{78}Si_{22}$) by neutron diffraction, and have suggested two types of trigonal prism structures. Figure 1(A) illustrates a trigonal prism capped with three half-octahedra (9 Pd atoms around a Si atom) and Fig. 1(B) illustrates a trigonal prism (6 Pd atoms around a Si atom). Ohkubo *et al.*[7)] have studied the structure of $Pd_{82}Si_{18}$ and $Pd_{75}Si_{25}$ by electron diffraction employing high-resolution electron microscopy (HREM) images. They have reported that the trigonal prism shown in Fig. 1(A) was major short-range order (SRO) of $Pd_{82}Si_{18}$ and $Pd_{75}Si_{25}$, because the coordination number of Pd atoms around a Si atom ($N_{SiPd}$) took nearly 9 by Reverse Monte Carlo modeling.

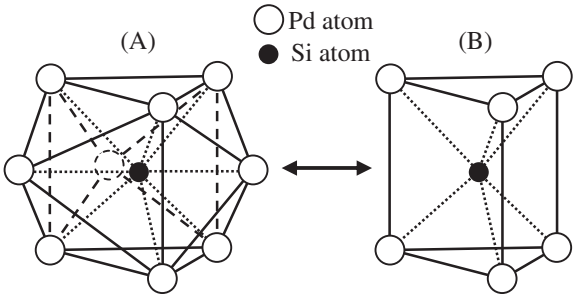


Fig. 1 Schematic illustrations of (A) trigonal prism capped with three half-octahedra (9 Pd atoms around a Si atom) and (B) trigonal prism (6 Pd atoms around a Si atom).[6)]

The effect of the trigonal prism on the thermal stability of metallic glassy alloys has been also studied. The trigonal prisms construct a cluster structure and the clusters form random cluster networks.[8)] Saida[9)] has suggested that the formation of trigonal prism clusters provides good stability of glass structure of metallic glassy alloys, because additional thermal energy is required to deconstruct the trigonal prisms and the clusters for glass transition. It follows from his study that the formation of trigonal prism clusters increases $T_g$.

The aim of this study is to determine the mechanism of the correlation between $T_g$ and the composition by measuring the structural parameters based on the SRO using Pd-Cu-Si metallic glassy alloy thin films. The mechanism was discussed on the standpoint of the formation of trigonal prisms.

## 2. Experimental

### 2.1 Alloy film preparation

Pd-Cu-Si thin films with seven kinds of compositions were deposited on glass substrates using an RF magnetron sputtering equipment (L-332FHS, Cannon ANELVA Corporation) with a simultaneous three sources (Pd, Cu and Si) sputtering mechanism and a substrates-rotating mechanism. The diameters of sputtering targets (Pd, Cu and Si) were 76.2 mm each. The rotation speed of substrates was fixed at 80 rpm. The substrate-target distance (S-T distance) was 70 mm. Ar-pressure for the sputtering was 0.3 Pa. The composition ratios of thin films were controlled by changing RF powers to the three kinds of sputtering targets individually. In order to fabricate Pd-Cu-Si alloys in amorphous phase, the three elements should be mixed homogeneously in a thin film. If a deposition rate (deposition thickness per one revolution of substrates) of an element is larger than its atomic diameter, it leads to the formation of a single element layer in principle. In order to obtain a structure of homogeneously mixed elements, a sparse deposition is required. Therefore, the RF power was controlled so that the deposition rate of each element became smaller than the corresponding atomic diameter. Deposition time for 4000 nm thick of thin films was calculated using the total deposition rates of three kinds of elements.

### 2.2 Alloy film characterization

The composition of fabricated thin films was analyzed by inductively coupled plasma-atomic emission spectrometry (ICP-AES). The glass transition temperature ($T_g$) and the exothermic peak corresponding to the crystallization of the alloys were measured with a differential scanning calorimeter (DSC, DSC6220, SII NanoTechnology Inc.). Ar gas was used for the atmosphere gas and the heating rate was 0.67 K/s. In order to examine the microstructure in the amorphous phase of the alloys indirectly, each thin film was allowed to heat to the corresponding peak-temperature at which the exothermic peak was indicated in DSC measurement. And then, the crystallized phase was determined with an X-ray diffractometer (XRD, RINT RAPID, Rigaku Corporation) using Cu K$\alpha$ radiation. The DSC was used to heat the thin films with the heating rate of 0.67 K/s in Ar gas atmosphere. After the heat-treatment, the thin films were cooled down quickly. The required time for cooling the sample from its peak-temperature to 500 K was about 5 min.

### 2.3 X-ray diffraction measurement

In order to determine the structural parameters based on the SRO of the thin films, synchrotron X-ray diffraction measurement was performed. The prepared thin films of about 4000 nm thickness were peeled off from glass substrates, and were cut into 9 mm square films. 40 pieces of the cut thin films were stacked in a stainless sample holder having two windows covered with polyimide films of 0.125 mm thickness, and the sample holder containing thin films was used for synchrotron X-ray diffraction measurement. The atmosphere in the sample holder was air at atmospheric pressure. The temperature during the measurement was about 293 K.

The synchrotron X-ray diffraction measurement was carried out using a horizontal two-axis diffractometer with a photon energy of 61.57 keV ($\lambda = 0.02014$ nm) at the BL04B2 beamline of the SPring-8 synchrotron radiation facility. After corrections for background, polarization, absorption and Compton scattering, the scattering intensity was normalized to give the structure factor, S($Q$), where $Q = 4\pi \sin\theta/\lambda$.[10]

## 3. Results and Discussion

### 3.1 Alloy film preparation and characterization

Table 1 shows the composition and $T_g$ of the thin films, samples (a) to (g), prepared by a sputtering method. Figure 2(A) shows DSC curves of the thin films. The glass transition temperatures ($T_g$) can be observed in all samples. This result proves all of the thin films are determined as metallic glassy alloys. Figure 2(B) shows XRD charts of the thin films heated to the corresponding peak temperatures at which exothermic peaks were indicated by DSC measurement. This result suggests the several correlations between the composition and the determined crystals. Samples (a) and (d) having high Cu content indicate the crystallization of $Cu_{0.6}Pd_{7.7}Si_{1.7}$. Samples (f) and (g) having high atomic ratios of Pd to Si indicate the crystallizations of Pd and $PdSi_5$. And also, the crystallizations of $Pd_3Si$ or $Pd_4Si$ are observed eventually in all samples. These crystals of $Pd_3Si$ or $Pd_4Si$ are supposed to be crystallized from the atomic arrangement of trigonal prisms. This result suggests that trigonal prisms are present as structural units in all samples.

The glass transition temperature ($T_g$) is plotted against Si and Cu content in Figs. 3(A) and (B), respectively. The positive effect of Si content on $T_g$ is observed in Fig. 3(A). The data in Fig. 3(B) are classified into three groups having similar Si content (Si = 18 at%, 14 at% and 12–13 at%) to eliminate the strong effect of Si content on $T_g$. Comparing the data in the same group, $T_g$ increases with increasing Cu content. The study on the effect of Cu content on $T_g$ has been reported by Chen.[11] He has measured $T_g$ of Pd-Cu-Si alloys with Si content fixed at 16.5 at% and Cu content ranging from 2 to 12 at%. In his study, $T_g$ increases with increasing Cu

Table 1 Composition and glass transition temperature ($T_g$) of prepared thin films.

| Sample | composition | $T_g, T$/K |
|---|---|---|
| (a) | $Pd_{67.8}Cu_{14.3}Si_{17.9}$ | 660 |
| (b) | $Pd_{75.1}Cu_{6.6}Si_{18.3}$ | 634 |
| (c) | $Pd_{81.8}Si_{18.2}$ | 638 |
| (d) | $Pd_{67.7}Cu_{18.2}Si_{14.1}$ | 627 |
| (e) | $Pd_{75.3}Cu_{10.3}Si_{14.4}$ | 623 |
| (f) | $Pd_{75.1}Cu_{12.3}Si_{12.6}$ | 614 |
| (g) | $Pd_{80.7}Cu_{6.9}Si_{12.4}$ | 591 |

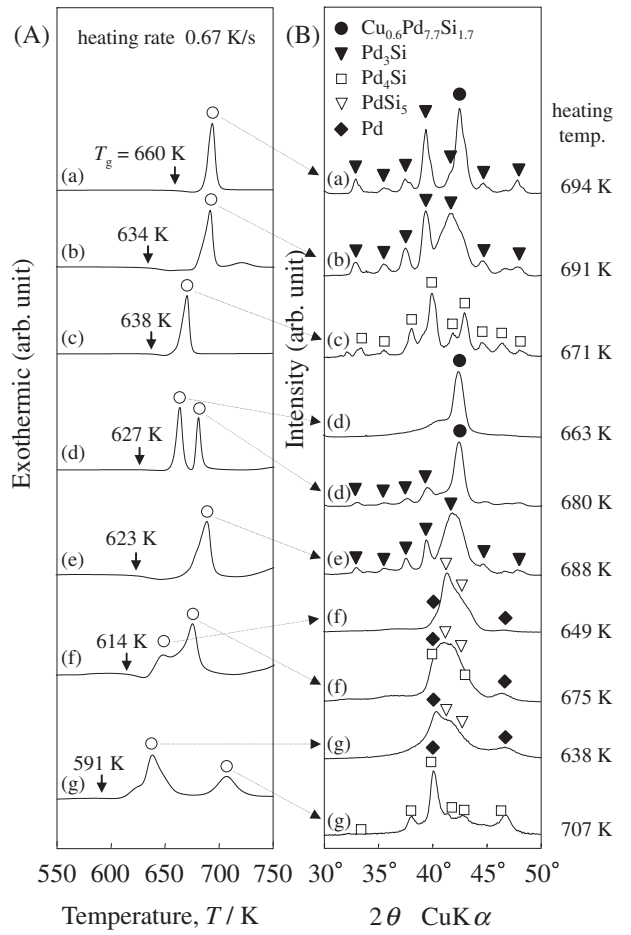


Fig. 2 (A) DSC curves of samples (a) to (g). (B) XRD charts of samples (a) to (g) heated to the corresponding peak-temperatures at which exothermic peaks were indicated by DSC measurement.

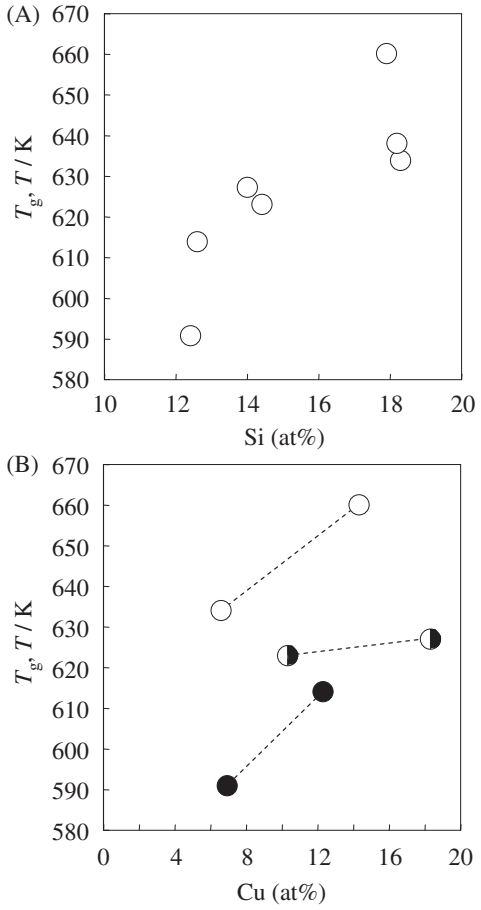


Fig. 3 Glass transition temperature ($T_g$) as a function of (A) Si content and (B) Cu content, respectively. (B) ○ Si = 18 at% ◑ Si = 14 at% ● Si = 12–13 at%

content. The result shows the same tendency as the obtained result in the present study.

### 3.2 X-ray diffraction measurement

In order to determine the mechanism of the correlation between $T_g$ and the composition, the structural parameters based on the SRO were measured.

Figure 4 shows the structure factors, $S(Q)$s, of samples (a) to (g) obtained by synchrotron X-ray diffraction measurement. The shoulder on the high $Q$ side of the second peak, which is a famous feature in the $S(Q)$ of amorphous alloys,[6] can be observed in all samples. Figure 5 shows the first peaks of radial distribution functions, RDF($r$)s, of samples (a) to (g). The RDF($r$)s are derived from the Fourier transformation of the corresponding $S(Q)$s truncated at $Q_{max} = 250\,nm^{-1}$. The method for deriving the RDF($r$) is explained in a Ref. 12).

In order to obtain the structural parameters based on the SRO of Pd-Cu-Si alloys, it is necessary to divide the first peak of RDF($r$) into partial correlations by the least square fitting with Gaussian functions. As an example of it, Fig. 6 shows the first peak of RDF($r$) of sample (b) with two Gaussian peaks ($r_1$ and $r_2$) indicating by broken lines. The two Gaussian peaks ($r_1$ and $r_2$) are corresponding to Pd-Si and metal-metal (Pd-Pd and Pd-Cu) pair correlations, respectively.

Pd-Cu-Si metallic glassy alloys have 6 kinds of pair correlations: Pd-Pd, Pd-Cu, Pd-Si, Cu-Cu, Cu-Si and Si-Si. However, we ignored the pair correlations of Cu-Cu, Cu-Si and Si-Si for the Gaussian peak-fitting, because their calculated weighting factors were very small. The weighting factor ($W_{ij}$) for the pair correlation between an $i$-atom and a $j$-atom is defined as follows:[12]

$$W_{ij} = \frac{c_i c_j f_i f_j}{\langle f \rangle^2} \tag{1}$$

$$\langle f \rangle^2 = \left( \sum_i c_i f_i \right)^2 \tag{2}$$

where $c_i$ and $f_i$ are the concentration and the atomic scattering factor of an $i$-atom, respectively. For example, the weighting factors of sample (b) $Pd_{75.1}Cu_{6.6}Si_{18.3}$ are calculated as follows: $W_{PdPd} = 0.784$, $2W_{PdCu} = 0.087$, $2W_{PdSi} = 0.116$, $W_{CuCu} = 0.002$, $2W_{CuSi} = 0.006$ and $W_{SiSi} = 0.004$.

For dividing the first peak of RDF($r$) into the Gaussian peaks corresponding to Pd-Pd, Pd-Cu and Pd-Si pair correlations, the peak positions should be fixed at first. As for the peak positions corresponding to Pd-Si and Pd-Pd pair correlations, several previous studies on structures of Pd-Si amorphous alloys have been reported, as we mentioned above. The structural parameters reported by Fukunaga

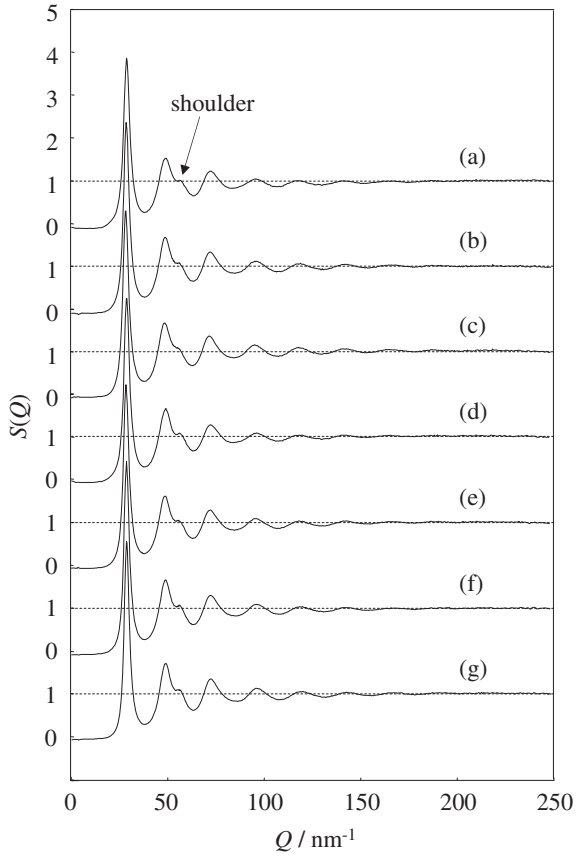


Fig. 4 Structure factors, $S(Q)$s, of samples (a) to (g).

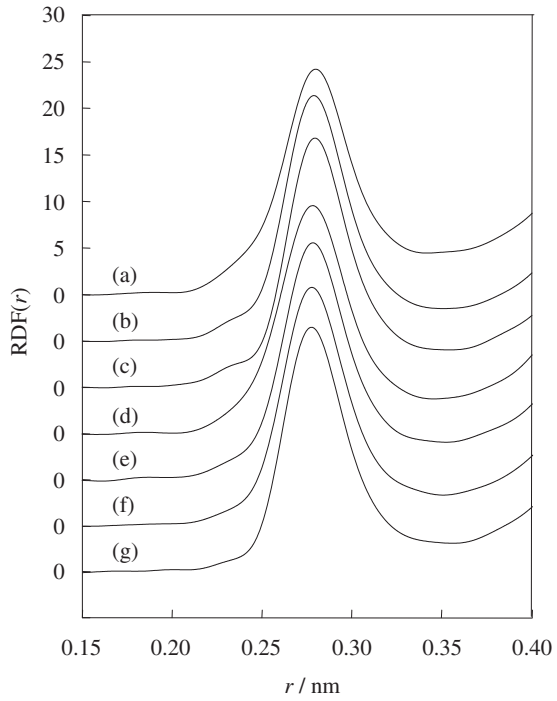


Fig. 5 First peaks of radial distribution functions, RDF($r$)s, of samples (a) to (g).

*et al.*[6] and Ohkubo *et al.*[7] are summarized in Table 2. The peak positions corresponding to Pd-Si and Pd-Pd are 0.242–0.248 nm and 0.275–0.281 nm, respectively. These peak positions are corresponding to $r_1$ and $r_2$ in Fig. 6,

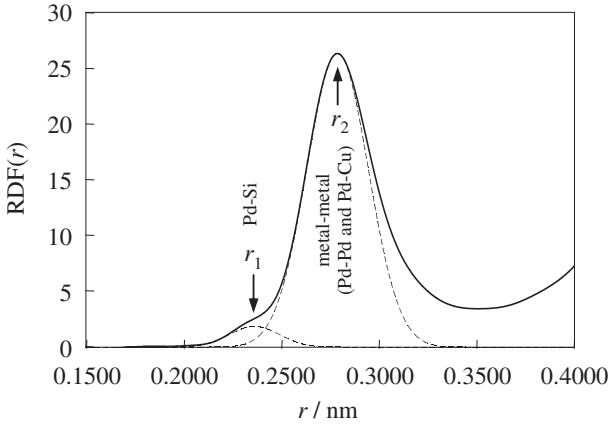


Fig. 6 The first peak of radial distribution function, RDF($r$), of sample (b). Broken lines are the Gaussian peaks corresponding to the Pd-Si and metal-metal (the Pd-Pd and Pd-Cu) pair correlations positioned at $r_1$ and $r_2$, respectively.

Table 2 Structural parameters of Pd-Si amorphous alloys reported in previous studies.[6,7]

| measurement | neutron diffraction[6] | | | electron diffraction[7] | |
|---|---|---|---|---|---|
| Glass sample | $Pd_{85}Si_{15}$ | $Pd_{80}Si_{20}$ | $Pd_{78}Si_{22}$ | $Pd_{82}Si_{18}$ | $Pd_{75}Si_{25}$ |
| Pd-Si position/nm | 0.242 | 0.242 | 0.243 | 0.242 | 0.248 |
| $N_{SiPd}$ | 7.3 | 6.6 | 6.3 | 9.1 | 8.8 |
| $N_{PdSi}$ | 1.2 | 1.6 | 1.8 | 2.0 | 2.9 |
| Pd-Pd position/nm | 0.278 | 0.280 | 0.281 | 0.275 | 0.279 |
| $N_{PdPd}$ | 10.5 | 10.6 | 10.1 | 12.1 | 11.0 |

respectively. The peak position is defined as the atomic distance between the pair of atoms. $N_{ij}$ expresses the coordination number of $j$-atoms around an $i$-atom.

The peak position corresponding to Pd-Cu pair correlation, which is defined as the Pd-Cu atomic distance, can be roughly estimated by calculating the sum of atomic radiuses of Pd atom and Cu atom. The atomic radiuses of Pd atom and Cu atom are 0.137 nm and 0.128 nm, respectively, thereby the peak position corresponding to Pd-Cu should be around 0.265 nm. Therefore, the Gaussian peak corresponding to Pd-Cu pair correlation should mainly belong to the $r_2$-positioned peak in Fig. 6.

However, we could not divide the $r_2$-positioned peak of RDF($r$) into two Gaussian peaks corresponding to Pd-Pd and Pd-Cu pair correlations by the calculated peak position of Pd-Cu. The atomic distance of Pd-Pd is around 0.28 nm from the previous studies[6,7] summarized in Table 2. The atomic distances of Pd-Pd and Pd-Cu are very close and additionally, $W_{PdPd}$ is much larger than $W_{PdCu}$. Therefore, the Gaussian peak of Pd-Cu will be so small that it will certainly be buried in the large peak of Pd-Pd completely. From this reason, we treated $r_2$ as the Pd-Pd atomic distance, although the $r_2$-positioned peak is corresponding to metal-metal (Pd-Pd and Pd-Cu) pair correlations.

For dividing the first peak of RDF($r$) into the Gaussian peaks, the peak position appearing at around 0.28 nm was assigned as $r_2$ at first and then, the Gaussian peak-fitting of $r_2$ was performed. After that, the Gaussian peak positioned at $r_1$ was fitted at around 0.24 nm.

Table 3 Peak positions ($r_1$ and $r_2$) and coordination numbers ($N_{ij}$) of samples (a) to (g) calculated from RDF($r$)s.

| Sample | composition | $r_1$/nm | $N_{PdSi}$ | $N_{SiPd}$ | $r_2$/nm |
|---|---|---|---|---|---|
| (a) | $Pd_{67.8}Cu_{14.3}Si_{17.9}$ | 0.2385 | 1.5 | 5.7 | 0.2797 |
| (b) | $Pd_{75.1}Cu_{6.6}Si_{18.3}$ | 0.2362 | 1.0 | 3.9 | 0.2788 |
| (c) | $Pd_{81.8}Si_{18.2}$ | 0.2330 | 0.9 | 3.9 | 0.2794 |
| (d) | $Pd_{67.7}Cu_{18.2}Si_{14.1}$ | 0.2380 | 1.1 | 5.5 | 0.2781 |
| (e) | $Pd_{75.3}Cu_{10.3}Si_{14.4}$ | 0.2340 | 0.7 | 3.7 | 0.2781 |
| (f) | $Pd_{75.1}Cu_{12.3}Si_{12.6}$ | 0.2324 | 0.6 | 3.6 | 0.2774 |
| (g) | $Pd_{80.7}Cu_{6.9}Si_{12.4}$ | 0.2300 | 0.3 | 1.8 | 0.2772 |

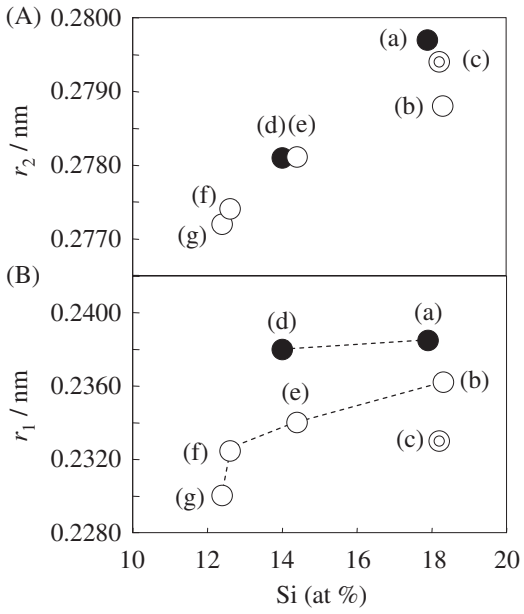


Fig. 7 Peak positions of RDF($r$)s, (A) $r_2$ and (B) $r_1$, as a function of Si content. ● Cu > 14 at% ○ Cu < 12 at% ◎ Cu = 0 at%

The coordination numbers ($N_{SiPd}$ and $N_{PdSi}$) were calculated using the area of the Gaussian peak positioned at $r_1$, weighting factors ($W_{PdSi}$ and $W_{SiPd}$) and the composition (Si and Pd content). The calculation method for them is explained in a Ref. 13).

The structural parameters ($r_1$, $r_2$, $N_{SiPd}$ and $N_{PdSi}$) of samples (a) to (g) were obtained by this procedure. They are summarized in Table 3. On the obtained structural parameters, it is to be noted that the Gaussian peak positioned at $r_1$ basically involves not only the Pd-Si pair correlation but the Pd-Cu pair correlation in no small part. Therefore, it is necessary to keep in mind that the peak position ($r_1$) and the coordination numbers ($N_{SiPd}$ and $N_{PdSi}$) calculated using the area of the $r_1$-positioned Gaussian peak will take excess values depending on the Cu content. From this reason, the data classification with Cu content was performed for the examination of the correlations between the composition and the structural parameters relating to the $r_1$-positioned Gaussian peak.

The correlations between Si content and the obtained structural parameters were examined. The peak positions ($r_1$ and $r_2$) are plotted against Si content in Figs. 7(B) and (A), respectively. The data are classified into three sample groups according to their Cu content (Cu > 14 at%, < 12 at% and = 0 at%) to eliminate the above mentioned effect of Pd-Cu pair correlation on the structural parameters ($r_1$, $N_{SiPd}$ and $N_{PdSi}$). The peak positions ($r_1$ and $r_2$) which are defined as the atomic distances of Pd-Si and Pd-Pd, respectively show positive correlations with Si content. These results are consistent with those of the previous studies by Fukunaga *et al.*[6] and Ohkubo *et al.*[7] (summarized in Table 2) indicating the positive correlations between the atomic distances (Pd-Si and Pd-Pd) and Si content. In Fig. 7(B), the peak positions ($r_1$) become larger with increasing Cu content due to the effect of the Pd-Cu pair correlation on the peak position ($r_1$).

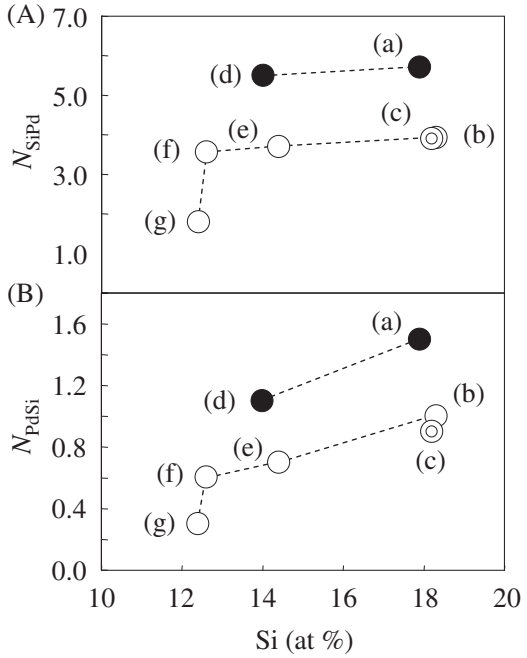


Fig. 8 Coordination numbers, (A) $N_{SiPd}$ and (B) $N_{PdSi}$, as a function of Si content. ● Cu > 14 at% ○ Cu < 12 at% ◎ Cu = 0 at%

The positive correlation between the peak position ($r_2$) and Si content can be explained as follows. As shown in Fig. 2(B), samples (f) and (g) having high Pd/Si ratios indicate the crystallizations of Pd and $PdSi_5$. From this result, the existences of Pd-nanocrystals can be expected in those samples. The atomic distance of fcc-Pd is 0.276 nm, which is shorter than the Pd-Pd atomic distances in Pd-Si amorphous alloys (0.275–0.281 nm) reported by the previous studies.[6,7] As we mentioned above, the formation of trigonal prisms is supposed in the samples of the previous studies. Additionally, it can be supposed that samples (f) and (g) have segregation phases, Pd-rich phase and Si-rich phase. The number density of a trigonal prism must be low in the structure having the segregation phases. Therefore, samples (f) and (g) indicate low $r_2$ due to Pd-nanocrystals in their structure, and the peak position ($r_2$) increases with increasing Si content due to the formation of trigonal prisms.

The coordination numbers ($N_{SiPd}$ and $N_{PdSi}$) of the three sample groups with different Cu content are plotted against Si content in Figs. 8(A) and (B), respectively. In Fig. 8(A), $N_{SiPd}$ indicates almost constant values or a slight increase against Si content except that of sample (g). This result is not consistent with those of the previous studies by Fukunaga

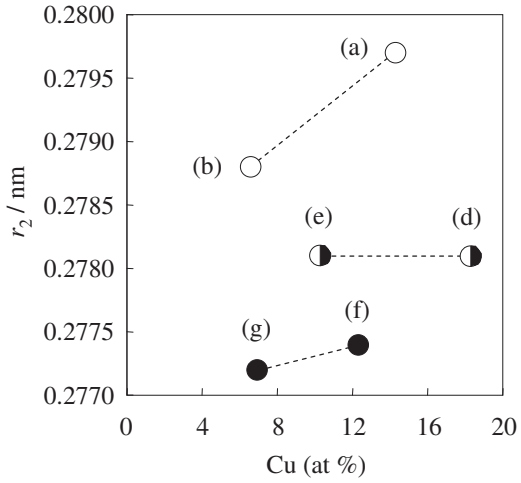


Fig. 9 Peak position ($r_2$) of RDF($r$)s as a function of Cu content. ○ Si = 18 at% ◑ Si = 14 at% ● Si = 12–13 at%

*et al.*[6] and Ohkubo *et al.*[7] showing the negative correlation between $N_{SiPd}$ and Si content. Fukunaga *et al.* explained the negative correlation by the transformation between two kinds of trigonal prisms illustrated in Figs. 1(A) and (B). They supposed that the trigonal prism structure unit (shown in Fig. 1(B)) was deformed to incorporate additional Pd atoms in its three tetragonal faces and finally a central Si atom had symmetrically 9 Pd atoms around it (shown in Fig. 1(A)), with decreasing Si content. The inconsistency of the correlations between $N_{SiPd}$ and Si content observed in this study and the previous studies is probably due to the segregation phases, Pd-rich phase and Si-rich phase, of samples (f) and (g). The segregation phases will decrease $N_{SiPd}$. In contrast, $N_{PdSi}$ shows the positive correlation with Si content in Fig. 8(B). This result is consistent with those of the previous studies by Fukunaga *et al.*[6] and Ohkubo *et al.*[7] showing the positive correlation between $N_{PdSi}$ and Si content.

In Figs. 8(A) and (B), the coordination numbers ($N_{SiPd}$ and $N_{PdSi}$) of the sample group with Cu content > 14 at% take larger values than those of the other groups due to the above mentioned effect of the Pd-Cu pair correlation on the coordination numbers.

The correlations between the obtained structural parameters and Cu content were examined. The peak position ($r_2$) is plotted against Cu content in Fig. 9. The reason of adopting the peak position ($r_2$) for examining the correlation is that $r_2$ is thought to be less affected by Pd-Cu pair correlation because of the large difference between $W_{PdPd}$ and $W_{PdCu}$. The data of sample (c) is not plotted, because only this sample has Cu-free composition. The data are classified into three sample groups having similar Si content (Si = 18 at%, 14 at% and 12–13 at%) to eliminate the strong effect of Si content on the peak position ($r_2$). The three sample groups show a zero or positive correlation between the peak position ($r_2$) and Cu content.

The correlations between the obtained structural parameters and the microstructure of Pd-Cu-Si metallic glassy alloys were discussed. Fukunaga *et al.*[6] have supposed that with increasing Si content, the three-dimensional arrangement of neighboring Pd atoms around a Si atom was likely to become more trigonal prismatic coordination in Pd-Si alloy glasses. From this theory, the change of the structural parameters with increasing Si content can be related to the change of the number density of trigonal prisms. In Table 2, the structural parameters, the atomic distances (Pd-Si and Pd-Pd) and $N_{PdSi}$, increase with increasing Si content. Therefore, it can be stated that this change in the structural parameters suggests an increase in the number density of trigonal prisms.

On the other hand, our results also indicate increases in the structural parameters, the atomic distances (Pd-Si and Pd-Pd) and $N_{PdSi}$, with increasing Si content. This result suggests that the number density of trigonal prisms increases with increasing Si content. Additionally, the result that the atomic distance of Pd-Pd increases with increasing Cu content suggests an increase in the number density of trigonal prisms. This result on Cu content is consistent with the result of a previous study. Nishi *et al.*[14] compared viscosity and activation energy of $Pd_{84}Si_{16}$ with those of $Pd_{78}Cu_6Si_{16}$, and obtained the result that $Pd_{78}Cu_6Si_{16}$ showed higher viscosity and activation energy than $Pd_{84}Si_{16}$. They supposed that the addition of Cu makes the construction of trigonal prism clusters easy, because Cu atoms coordinate as capping-atoms of a Pd-Si trigonal prism, and two Pd atoms and one Cu atom make a new basic plane of a new trigonal prism.

The positive correlation between $T_g$ and the number density of trigonal prisms can be derived from the obtained positive correlations between $T_g$ and the composition (Si and Cu content) in Fig. 3 and between the number density of trigonal prisms and the composition (Si and Cu content) in Figs. 7, 8 and 9. The derived positive correlation between $T_g$ and the number density of trigonal prisms is consistent with the theory of Saida[9] which we mentioned before: the formation of trigonal prism clusters increases $T_g$.

The obtained results can be concluded as follows. Si and Cu content have positive effects on the formation of trigonal prisms in the structures of Pd-Cu-Si metallic glassy alloys. Those effects can be confirmed by the change of the structural parameters: the Pd-Si atomic distance, the Pd-Pd atomic distance and $N_{PdSi}$. Furthermore, the formation of trigonal prisms has a positive effect on increasing $T_g$.

## 4. Summary

In this study, Pd-Cu-Si metallic glassy alloy thin films were fabricated by sputtering method, and the effect of the composition on $T_g$ was examined. In order to determine the mechanism of the obtained effect, the structural parameters of the thin films based on the short-range order (SRO) were measured, and the correlations between them and the composition were examined. The mechanism was discussed on the standpoint of the formation of trigonal prisms. The obtained results are summarized as follows.

(1) Glass transition temperature ($T_g$) increased with increasing Si and Cu content.

(2) The atomic distances (Pd-Si and Pd-Pd) and the coordination number of Si atoms around a Pd atom ($N_{PdSi}$) increased with increasing Si content. Additionally, the Pd-Pd atomic distance increased with increasing Cu content.

These results suggest that Si content and Cu content have positive effects on the formation of trigonal prisms in the structures of Pd-Cu-Si metallic glassy alloys.

(3) From these obtained correlations, it can be concluded that $T_g$ increases with an increase in the number density of trigonal prisms. Therefore, an increase in $T_g$ with increasing Si and Cu content is supposed to be caused by the composition dependent formation of trigonal prisms.

## Acknowledgments

The authors would like to thank Dr. K. Ohara for his assistance in X-ray diffraction measurement. The synchrotron radiation experiments were approved by the Japan Synchrotron Radiation Research Institute (proposal numbers: 2008B1074 and 2009A1078).

## REFERENCES

1) U.S. Department of Energy: Fuel Cells, Technical Plan, Multi-Year Research, Development and Demonstration Plan, (2007).
2) H. S. Chen and D. Turnbull: Acta Metall. **17** (1969) 1021–1031.
3) S. Kajita, S. Yamaura, H. Kimura, K. Yubuta and A. Inoue: IEE Trans. SM **128** (2008) 225–229.
4) S. Kajita, S. Yamaura, H. Kimura, K. Yubuta and A. Inoue: Sens. Actuators B **150** (2010) 279–284.
5) A. Inoue: Acta Mater. **48** (2000) 279–306.
6) T. Fukunaga and K. Suzuki: Sci. Rep. Inst. Tohoku Univ. A **29** (1981) 153–175.
7) T. Ohkubo, Y. Hirotsu and M. Matsushita: J. Electron Microsc. **48** (1999) 1005–1013.
8) T. Takeuchi, D. Fukamaki, H. Miyazaki, K. Soda, M. Hasegawa, H. Sato, U. Mizutani, T. Ito and S. Kimura: Mater. Trans. **48** (2007) 1292–1298.
9) S. Saida: *New Functional Materials, Fundamentals of Metallic Glasses and their Applications to Industry*, (TECHNOSYSTEM, Japan, 2009) p. 33.
10) S. Kohara, M. Itou, K. Suzuya, Y. Inamura, Y. Sakurai, Y. Ohishi and M. Takata: J. Phys.: Condens. Matter **19** (2007) 506101.
11) H. S. Chen: Acta Metall. **22** (1974) 1505–1511.
12) T. Fukunaga: *JIM Seminar Text* 73, (THE JAPAN INSTITUTE OF METALS, Japan, 1997) p. 107.
13) Y. Waseda and E. Matsubara: *X-ray Structure Analysis*, (UCHIDA ROKAKUHO PUBLISHING CO., LTD., Japan, 1998) p. 213.
14) Y. Nishi, N. Kayama, S. Kiuchi, K. Suzuki and T. Masumoto: J. Japan Inst. Metals **44** (1980) 1336–1341.